Optimal damping factor for the Least Squares inverse Kinematics for the Steam Generator Inspection System

S. Joseph Winston [1], P.V. Manivannan [2]

[1] Steam Generator Inspection Devices section,
Indira Gandhi centre for Atomic Research, Kalpakkam
winston@igcar.gov.in

[2] Department of Mechanical Engineering,
Indian Institute of Technology-Madras, Chennai 600036
pvm@iitm.ac.in

Abstract

The Steam Generators used in the Prototype Fast Breeder Reactor have sodium on shell side and water/steam on the tube side. Tube inspection and qualification of all 547 tubes, enhances the safety and reduces the operation cost by increasing plant availability. In this work, a two axis planar reach robotic arm called as Tube Locator Module (TLM) is used for reaching and orienting the Remote Field Eddy Current (RFEC) testing probe at the exact location of individual Steam Generator tube and the probe is pushed through the entire tube length for inspection and qualification of the same. A conventional method of inverting the Jacobian and using a pseudo inverse will help in running the actuators in joint space to reach the desired position of the end effector. However, as pseudo inverse suffers numerical stability close to singularities of the manipulator, hence it is proposed to use the damped least squares pseudo inverse method by introducing a damping factor to improve the stability. Higher damping factor increases the stability of manipulator, even when the manipulator moves closer to its to singular configurations. However, higher damping factors lead to more tracking error in the end effecter trajectory. Hence in this work, based on the tracking errors and the geometrical constraints, an optimal damping factor is arrived at for the smooth motion of the TLM. This paper also deals with the manipulability study of the TLM to understand the singular configurations and apply the damping factor to stabilize the joint angular velocities without causing much error in the end effector trajectory.

Keywords: PFBR, SG, Inspection, Manipulator, Inverse kinematics, DH parameter, Forward Kinematics, Yoshikawa manipulability, tracking error.

1 Introduction

In Prototype Fast Breeder Reactor (PFBR), there are 8 Steam Generators (SG), each having 547 tubes in bundle carrying water/steam inside and sodium surrounds the tube in the shell side. As sodium water reaction is exothermic, it is highly undesirable to have a breach in the SG tubes. This mandates a stringent qualification of the SG tubes, by checking for any flaws (or) wall thinning prior to commissioning and also during maintenance operation. Ferritic steel is used to make the SG tubes, due its inherent ability to withstand Stress Corrosion Cracking (SCC), in addition to its high thermal conductivity. However, since ferritic steels are ferromagnetic in nature, only the Remote Field Eddy Current (RFEC) probe can be used for inspecting the tubes.

Lot of effort has been put all over the world towards development of remote inspection systems [1] for SG tube qualifications using RFEC probe, along with necessary data acquisition system. International experiences reveal that the plant availability for power generation depends highly on the SG availability. Hence, the efforts are to increase the plant availability with due importance to the plant safety through proper tube inspections and qualifications. A two-axis precision robotic manipulator is designed to orient the end effector to all the 547 tubes uniquely for locating the steam tubes and to push the probe into the tubes for inspection. The kinematic algorithm developed is programmed and simulated using the Python language. The position kinematics and velocity kinematics have been implemented for a point to point (tube to tube) movement of the device. The singular configurations are understood for the TLM and a strategy of increasing the stability of the numerical solution has been adapted through the implementation of the Damped Least Squares pseudo inverse method. A detailed study has been performed to compare the tracking error of the TLM end effector due to the damping factor. An optimal damping factor has been arrived, so that the device has least tracking error with highest stability close in region of the singularity configurations of the TLM. After the simulating the system using Python scripting language, the same methodology has been implemented on the commercially available ELMO motion controller, which facilitates the coding through Structured Text (ST) complying with the IEC 61131-3 OpenPLC coding format to run and check in the actual system.

2 Tube Locator Module (TLM)

Since the tube sheet is planar, a typical Selective Compliant Assembly Robotic Arm (SCARA) type device called as Tube Locator Module (TLM) is designed (Fig.1). The DH parameters of the TLM is given in the Table.1.

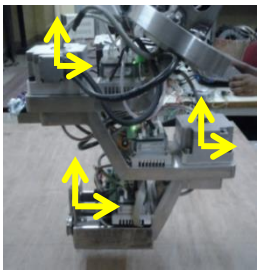

Fig.1 Tube Locator Module

Table.1 DH parameters for TLM

Joint No (i)	θ_i	α_i	χ_i	d_i
0	$\theta_{shoulder}$	0	210.0	115.0
1	θ_{elbow}	0	210.0	115.0

The geometry of TLM is designed such that it can be assembled into the inclined manhole of SG. The TLM unfolds into the header during the deployment, to reach all the row tubes covering a radial distance of 420mm. It becomes a prime importance to do the kinematic analysis of the manipulator, to estimate the singular configuration for mitigating the sudden accelerations / jerks. The arm motion becomes highly unstable, when it is close to the singular pose. This is due to large change in the joint space angles for small change in the end effector Cartesian space moves, which causes undesirable arm motor tripping due to over currents. The best way to estimate the closeness to the singular configuration is to properly analyze the manipulator

Jacobian. It is also evident that this singular configuration is independent of the first joint (shoulder) angle.

3 Inverse Kinematics for TLM

In order to avoid singularity, a Damped Least Squares (DLS) [2] inverse kinematics methodology has been followed. Formulating the inverse of Jacobian through a pseudo inverse using the DLS method provides good system stability close to its singular configuration. However, as the damping factor increases, the tracking error of the manipulator also increases. Hence, to find the optimal damping factor that results in minimum tracking error, a kinematic algorithm is coded in python scripting language. Simulation were carried out for finding the reachability of end effector in the given task space. To study the behaviour of the arm close to its singular configurations, the arm is made to move from the coordinate [420.0,0.0] to [-420.0,0.0] (both are singular configuration points of the SG tube sheet). This point to point movement makes the manipulator to start close from its first singular configuration and move through the vicinity of centre tube with [0.0,0.0] coordinate (which is also a singular configuration point) and reach the destination. The best way to estimate the closeness to a singular configuration is to estimate the manipulability of the manipulator. The Yoshikawa manipulability [3,4] is computed to define the condition of the Jacobian at every kinematic step. Since, the tubes are in a hexagonal array form, a numbering scheme has been evolved to obtain the coordinate values, if the user selects the row number and tube number in the array. The Fig.2 shows the numbering scheme adapted for the SG tube sheet. Equations 1 & 2 show the tube centre coordinates in Polar and Cartesian coordinate system respectively.

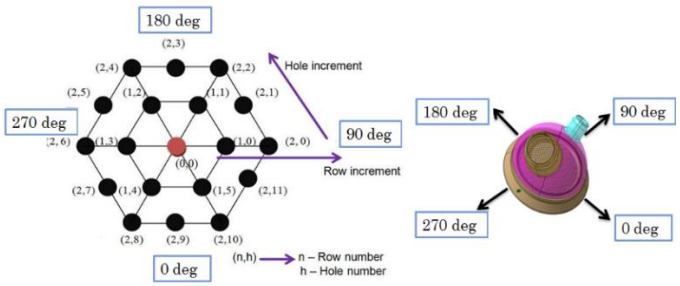

Fig.2 SG tube ordering scheme (Hexagonal array pattern)

$$(r,\theta) = \left(a\sqrt{n^2 + h^2 - nh}, \cos^{-1}\left(\frac{a(2n-h)}{2r} \right) \right) \tag{1}$$

$$\begin{bmatrix} x \\ y \end{bmatrix} = \begin{pmatrix} r\cos\theta \\ r\sin\theta \end{pmatrix} \tag{2}$$

where, '*r'* and Θ are polar coordinates of the tube centers, '*a*' is tube pitch, '*n'* is row number, '*h'* is tube number in the row. The joint space variables are related to the end effecter position (in Cartesian space coordinates) through the Jacobian matrix.

Generally, when the Jacobian matrix is a non-square matrix, a pseudo inverse is carried out to obtain the inversion of Jacobian. The forward kinematics shows the end effecter position is a function of joint space variables, which is expressed by the Eq.3. Its inverse kinematics expression given by Eq.4.

$$[e] = J[\theta] \tag{3}$$

$$[\theta] = J^{-1}[e] \tag{4}$$

The Jacobian matrix (J) in the above equation is an m X n- matrix, where 'm' represents the DOF of the manipulator and 'n' represents independent joints in the manipulator. When 'm' is not equal to 'n', a pseudo inverse technique is implemented to find the inverse of Jacobian. In all practical cases, to mitigate the stability issue, when the manipulator end effector is close to the singular position, the Damped Least squares (DLS) Jacobian Inverse ($J^{\dagger}$) [2] is used and is mathematically represented by Eq.5.

$$J^{\dagger} = J^{T}(JJ^{T} + \lambda^{2}I)^{-1} \tag{5}$$

where, 'λ' is a damping factor [6,7]. When the value of λ =0, the inverse of Eq.5 will typically work as a pseudo inverse. Further, this 'λ' strengthens the diagonal elements of Jacobian near manipulator's singular positions, by reducing the tendency of matrix to have determinant value equalizing zero. Implementing DLS induces the deviation in tracked path from shortest path; but simultaneously improving stability at singular positions.

The velocity kinematics [8] can be implemented as follows,

$$\left[\dot{\theta}\right] = J^{\dagger}\left[\dot{e}\right] \tag{6a}$$

$$\left[\Delta\theta\right] = \left[\dot{\theta}\right]\left[\Delta t\right] \tag{6b}$$

$$\left[\theta_{i+1}\right] = \left[\theta_{i}\right] + \left[\Delta\theta\right] \tag{6c}$$

Where, θ is joint angle vector and 'e' is change in end effector position in the given time interval. In order to have a good linearization, the discrete time step is chosen with smaller interval, so that the joint angles and end effector position changes with smaller steps. This is implemented to reduce large change in joint velocities, when higher times are used, that will mask the velocity changes due to manipulability near the singular configurations.

4 Manipulability study for TLM

Manipulability is a measure of the ability of the manipulator to move in specific directions. This study is important, as the manipulator close to its singular configurations will have very less ability to move in specific directions and requires very large torque for motion. This results in motors drawing more current. In addition, the velocities have a sudden spike causing a lot of accelerations in the manipulator arms, producing undesirable dynamic forces in the system.

Considering, a set of joint velocities with constant unit norm i.e., a unit sphere in the joint velocity space given in Eq.7

$$\dot{q}^T \dot{q} = 1 \tag{7}$$

If v_e is the end effecter velocity in Cartesian space, the joint velocity is given by the following expression:

$$\dot{q} = J(\theta)^{\dagger} v_e \tag{8}$$

Now, the Eq 7 now becomes:

$$\left[J(\theta)^{\dagger} v_e \right]^T \left[J(\theta)^{\dagger} v_e \right] = 1 \tag{9}$$

where, pseudo inverse is as follows,

$$J(\theta)^{\dagger} = J(\theta)^T \left[J(\theta) J(\theta) \right]^{-1} \tag{10}$$

Simplifying the Eq 9, we get,

$$v_e^T \left[J(\theta) J(\theta)^T \right]^{-1} v_e = 1 \tag{11}$$

The expression above defines the points on the surface of an ellipsoid in the end-effector velocity space. The shape and size of the ellipsoid is given by the Eigen decomposition of the matrix $J(q)J(q)^T$. For a 2R manipulator, the ellipsoid becomes an ellipse. The directions of the principal axes of the ellipse is given by the direction of the eigenvectors of $J(q)J(q)^T$ and the lengths of the axes of the ellipse by the square root of the eigenvalues. In the case of a planar manipulator, as in the case of TLM, the $J(q)J(q)^T$ has two orthogonal eigenvectors with corresponding its Eigen values.

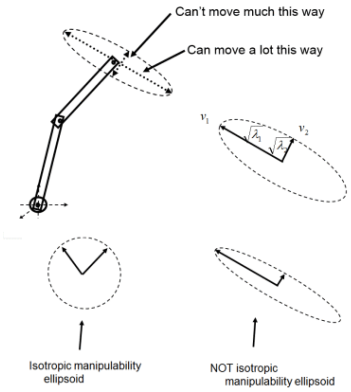

Fig.3 Manipulability ellipse

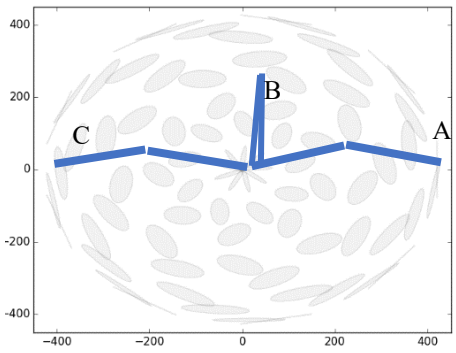

Fig.4 Manipulability on the task space

The Fig.3 shows the manipulability ellipse of the TLM. The direction of major and minor axes is given by corresponding Eigen Vectors, while their magnitude is given by Eigen values. The Fig.4 shows the manipulators velocity manipulability of TLM in its task space. It also shows three configurations A, B & C, which are close to singular poses. A large diagonal scalar value (i.e. Eigen value) indicates high manipulability in the corresponding direction. The condition number in Eq. 12 , k - is defined as the ratio of the smallest and largest Eigen value of $J(q)J(q)^T$ matrix. If the value of the condition number (k) is close to unity, we have an isotropic ellipse (which is a circle). On the other hand, if the value of 'k' is either very small (or) high, it indicates that the manipulator is close to its singular point. Having an isotropic ellipse is preferable, as it indicate good manipulability in all directions. The condition number k is given as:

$$k = \sqrt{\frac{\lambda_2}{\lambda_1}} \tag{12}$$

Where λ_1 and λ_2 are major and minor axis of ellipse. The area of the ellipse gives the manipulability index. The Manipulability index, μ is given as,

$$\mu = \sqrt{\left|J(\theta)J(\theta)^T\right|} \tag{13}$$

For a 2R planar manipulator, as in the present case of TLM, the manipulability is independent of the first joint angle (i.e. the shoulder angle) [9]. This is indicated through Eq.16. The end effecter function for a 2R planar can easily be written as follows;

$$e = \begin{bmatrix} e_x \\ e_y \end{bmatrix} = \begin{bmatrix} l_1 \cos\theta_1 + l_2 \cos(\theta_1 + \theta_2) \\ l_1 \sin\theta_1 + l_2 \sin(\theta_1 + \theta_2) \end{bmatrix} \tag{14}$$

The Jacobian matrix is calculated as;

$$J(\theta) = \begin{pmatrix} -l_1 \sin\theta_1 & -l_2 \sin(\theta_1 + \theta_2) \\ l_1 \cos\theta_1 & l_2 \cos(\theta_1 + \theta_2) \end{pmatrix} \tag{15}$$

The manipulator will be in a singular configuration, when the determinant of Jacobian becomes zero;

$$\therefore \left|J(\theta)\right| = l_1 l_2 \sin\theta_2 \tag{16}$$

It is obvious from the Fig.4, the manipulability ellipse tends to a straight line, when the elbow arm aligns with the shoulder arm. Hence, the manipulator suffers from velocity manipulability in that particular directions. This configuration of manipulator can be generalized as:

$$\theta_2 = \{n\pi : n\varepsilon N\} \tag{17}$$

In the TLM work space, the central and peripheral tubes locations gives rise to manipulability. However, a considerable effort has been put to handle this manipulability, when the manipulator pose is close to A, B (or) C, as shown in Fig.4. The same figure gives us the understanding for choosing any two point diametrically opposite to study the manipulability; which will be a worst case scenario. Further, due to circular symmetry, the manipulability will be same for all angles in the polar space of the TLM in diametrical direction motions.

5 Effect of damping factor

In order to study the manipulability and the tracking error, Inverse kinematics algorithm has been developed in the computer scripting language - Python. Python has been chosen, as it has many library routines to graphically represent the results easily through plots. It also has the Linear Algebra routines as a built-in library.

5.1 Simulation through Python

The algorithm uses the DH parameters as input data. Using forward kinematics method, the position of the end effector is calculated. The Inverse kinematic algorithm computes the joint space values for the movement of end effector from present position of the end effector to goal position. The joint space parameters (joint

angular positions and velocities) are computed in discrete steps. After each step movement, the code re-computes the Jacobian matrix for further inversions in an iterative scheme

Once the IK code is functional, the velocity manipulability is computed in every discrete step to analyze the manipulators configuration for further motion towards the target goal point [10]. In our case study, it has been chosen to start the end effector position from close to [420.0,0.0] and move to position [-420.0,0.0] by passing through the center singular point [0.0,0.0].

The Table.2 shows the manipulability, manipulability Index and the Eigen values at the point closer to [420.0,0.0]. The manipulability 'μ' and the manipulability index as discussed earlier are computed for various damping factors 'λ'. It can be noticed that the increase in damping factor results in increase area of the ellipse i.e. shown as 'μ'. The Manipulability index close to unit indicate a configuration, where the manipulator will have isotropic manipulability. A higher or lower value shows least manipulability in the particular directions. It is also obvious from the Eq.17 that the manipulator position with elbow angle θ_2 is equal to 0 and π, the manipulator is close to the singularity condition.

Table.2 Manipulability close to the first singular point A [420.0,0.0]

$\boldsymbol{\lambda}$	$\boldsymbol{\mu}$	$\boldsymbol{k = \sqrt{\frac{\lambda_1}{\lambda_2}}}$	$\boldsymbol{\lambda_1}$	$\boldsymbol{\lambda_2}$
0	1539.1	20513.9	220435.5	10.7
20	9524.0	537.6	220835.5	410.7
40	18911.4	137.8	222035.5	1610.7
60	28441.8	62.0	224035.5	3610.7
100	48029.5	23.0	230435.5	10010.7
200	102079.5	6.5	260435.5	40010.7

Table.3 Manipulability close to the second singular point B [0.0,0.0]

$\boldsymbol{\lambda}$	$\boldsymbol{\mu}$	$\boldsymbol{k = \sqrt{\frac{\lambda_1}{\lambda_2}}}$	$\boldsymbol{\lambda_1}$	$\boldsymbol{\lambda_2}$
0	769.7	3283.1	44100.0	13.4
20	4289.3	107.6	44500.0	413.4
40	8586.8	28.3	45700.0	1613.4
60	13128.6	13.2	47700.0	3613.4
100	23275.0	5.4	54100.0	10013.4
200	58009.7	2.1	84100.0	40013.4

Table.4 Manipulability close to the second singular point C [-420.0,0.0]

$\boldsymbol{\lambda}$	$\boldsymbol{\mu}$	$\boldsymbol{k = \sqrt{\frac{\lambda_1}{\lambda_2}}}$	$\boldsymbol{\lambda_1}$	$\boldsymbol{\lambda_2}$

0	384.8	328277.2	220496.0	0.7
20	9407.8	551.3	220896.0	400.7
40	18854.8	138.8	222096.0	1600.7
60	28405.9	62.2	224096.0	3600.7
100	48011.6	23.0	230496.0	10000.7
200	102078.5	6.5	260496.0	40000.7

The Table.3 shows the manipulability for various damping factor at $\theta_2 = \pi$, i.e. the end effecter is at position [0.0,0.0]. Similarly, the Table.4 shows the manipulability variation close to the singular configuration 'C', i.e. when the end effecter reaches the position [-420.0,0.0]. The angular velocities shoot up close to the singular configuration and at times show discontinuities which causes the joint motors to trip due to severe accelerations and jerks. The Fig.5 shows the joint angular velocities. The linear speed of the end effecter in Cartesian space is limited to uniform 20 mm/s from the safety concerns of device. The Fig.5 clearly indicates the high change in motor speeds at configurations A, B and C. The figure also indicates the smoothening of the velocity curves at higher damping factors. At zero damping factor, the system will become highly unstable, when manipulator reaches close to singular configuration. This is evident from Fig.5, as the angular velocities of the joints reaches close to 5 radians/s, which is very high and it may cause the motor tripping.

5.2 Manipulability

Once, the IK code is functional, the velocity manipulability is computed in every discrete step to analyze the manipulators configuration for further motion towards the target goal point. Similar to previous case study, it has been chosen to start the end effector position from close to [420.0,0.0] and move to position [-420.0,0.0] by passing through the center singular point [0.0,0.0].

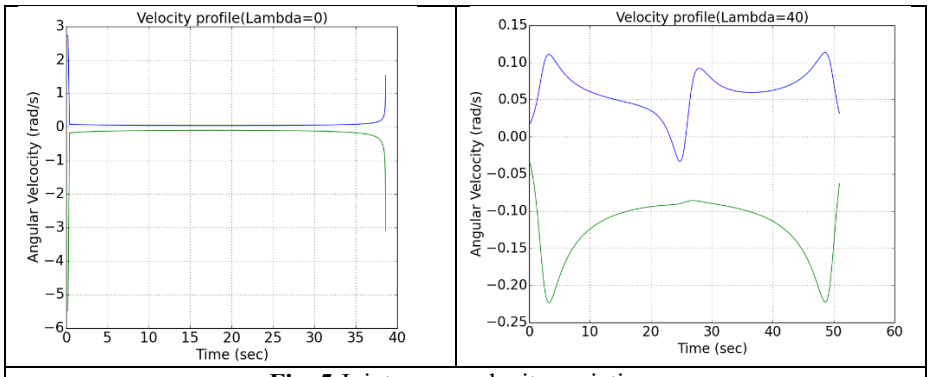

Fig. 5 Joint space velocity variations

5.3 Tracking error

The tracking error is a measure of deviation of actual end effecter path compared to the desired path of the TLM. From the IK solution, the joint angles at various time

steps are used to construct the end effector path by running the forward kinematic routine. The best way to express tracking error is by finding the area enveloped by the end effecter from the shortest straight line path.

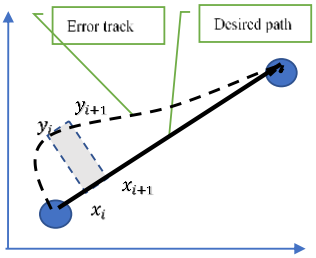

Fig.6 Error quantification

This algorithm is also coded in Python. First, it computes the vector angle subscribed between the start to end point line and the X-axis. The end effecter tracking points is rotated to reference x-axis, so that area integration is easy. This is done by a transformation matrix with rotation angle equal to the computed vector angle. The peak error indicates the peak value of the deviated track of the end effecter and the area indicates, how much deviant was the tracking as compared to the original shortest path between point to point move of the manipulator as shown in Fig. 6. The Eq.18 shows the area integration of the deviated path from the desired path.

$$Tracking\ Error = \sum_{i=1}^{n} \left(x_{i+1} - x_i\right)\left(\frac{y_{i+1} + y_i}{2}\right) \tag{18}$$

where 'x' is the displacement along the shortest path between the initial and the goal point, while 'y' is the perpendicular deviation from the desired trajectory (shortest path). Figure 7 shows the tracking error plot for damping factors 40 and 200. The Fig. 8 shows that the peak error and tracking error measured as area and trend of the curves almost matches. This indicates that the tracking is smooth without sudden spikes. It is quite obvious that for very high damping factors, the tracking error values are very high. This shows that increasing the damping factor beyond the optimal value will give rise to undesirable tracking errors.

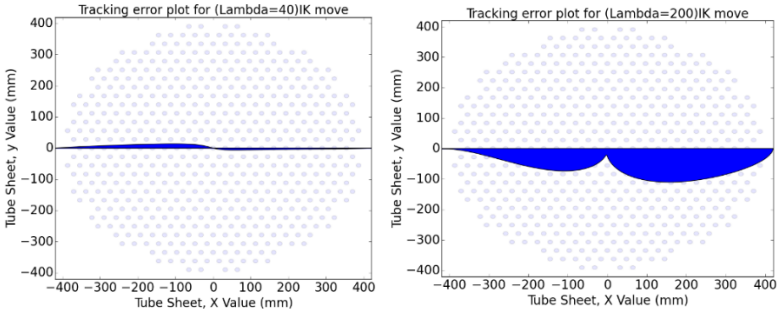

Fig.7 Tracking error for various damping factors

5.4 Optimal damping

It is obvious from the foregoing analysis that the increase in damping factor increases the manipulator's stability. Further, the increase in damping factor reduces

the peak angular velocities of the motor in proximity to the singular configuration of the manipulator. However, with high damping factor, the tracking error also increases. Especially in the SG inspection, if some tubes are plugged (i.e. defecting tubes of the steam generator are normally closed using plugs), the plug head will project up from the tube sheet. Hence, due to excess tracking error, the inspection probe at the manipulator end effecter may deviate from planned path and come in contact with plugs and cause undesirable collisions which will damage the probe. Therefore, to optimize the damping factor for the manipulator, TLM, the peak angular velocities estimated close to the singular points at A and C (in Fig.4) for various damping factors are compared against the tracking error of the manipulator as shown in Fig. 9. The crossover of these two curves (namely: tracing error & angular vs. damping factor) happen close to the damping factor 35. However, for a damping factor (λ) of 40, though the tracking error is slightly higher (which is acceptable because of large tube – tube pitch), the peak angular velocity is lower; thereby improving the stability. Hence, damping factor of 40 has been chosen as the optimal value for the Damped Least squares (DLS) pseudo inverse algorithm for the TLM manipulator.

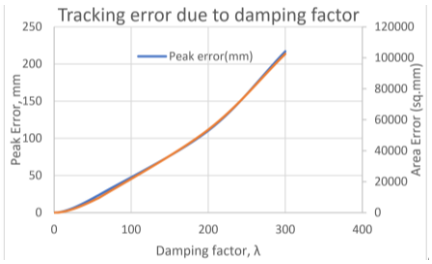

Fig.8 Tracking error due to Damping factor, λ

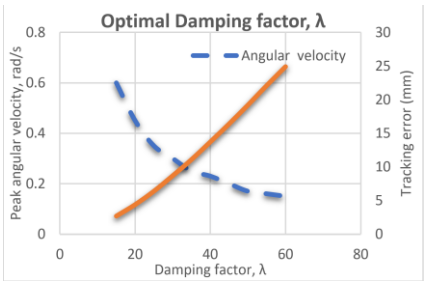

Fig.9 Optimal damping factor,λ

6 Implementation on motion controller

The DLS IK algorithm is programmed on the commercially available motion controller, Elmo. The coding is done through the open standard, IEC 61131-3 OpenPLC coding syntax, ST code and Functional Block Diagrams (FBD). The manipulator is fixed on a test stand as shown in Fig. 10. The system has been under various conditions and found to be highly stable even close to the singular configurations. Also, the tracking error is found to be well within the allowable limits. Hence, the optimal damping factor chosen as 40 is a good choice. It is also ensured through the implementation of the DLS methodology, the convergence to the IK solution, tracking error are within in the allowable limits. This protects the system from any abnormal motor trips and also maintains a highest stability even close to its singular configurations. Subsequently, the device has performed well during the actual inspection campaign on 8 PFBR SGs without any single motor trips.

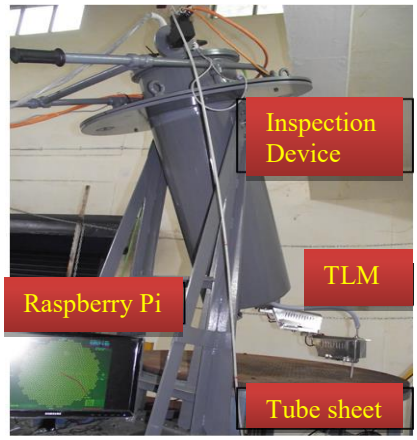

Fig. 10 Experimental setup

7 Conclusion

Steam Generator of Fast Breeder reactors need the qualifications of the tubes, in order to reduce operational costs by attaining highest plant availability. A versatile remote tube inspection manipulator (TLM) has been designed. We have also developed required forward and inverse kinematics algorithms, in addition to routines necessary calculating the optimal damping factor. From the simulation studies, it has been found that higher damping factor leads to better manipulator stability; however it leads to undesirable tracking error. It has been found that a damping factor (λ) value of: 40 results in smooth motion of end effector motion, with minimal tracking error. This methodology has been implemented on a commercial motion controller ELMO and checked for stability and tracking error deviation. The experimental study indicates that system performs well, even close to its singular configurations. Subsequently, the device has performed well during the actual inspection campaign on 8 PFBR SGs without any single motor tripping. This not gives assurance but gives utmost safety as the tube to tube motion is simulated prior to the actual motion on the robotic arm through manipulability and error estimations through the motion controller.

References

[1] L. Obrutsky, J. Renaud and R. Lakhan, “Steam Generator Inspections: Faster, Cheaper And Better, Are We There Yet?“, IV Conferencia Panamericana de END, Buenos Aires – Octubre 2007.

[2] Samuel R. Ross, “Introduction to Inverse Kinematics with Jacobian Transpose, Pseudoinverse and Damped Least Squares method”, Department of Mathematics, University of California, San Diego, October 7, 2009.

[3] TsuneoYoshikawa, “Foundation of Robotics-Analysis and Control, Corona Publication Pvt. Ltd, Japan, PP127-153

[4] T. Yoshikawa, “Manipulability of Robotic Mechanisms”, International Journal of Robotics Research, vol. 4, 1985

[5] Jazar, Reza.N, "Theory of Applied Robotics-Kinematics, Dynamics, and Control (2nd Edition)", Springer

[6] S. Chiaverini, B. Siciliano and O. Egeland, Review of the damped least-squares inverse kinematics with experiments on an industrial robot manipulator, Control Systems Technology, IEEE Transactions on, 2 (1994) 123-134.

[7] Le Minh Phuoc, Philippe Martinet ,Sukhan Lee and HunmoKim,"Damped least square based genetic algorithm with gaussian distribution of damping factor for singularity-robust inverse kinematics", Journal of Mechanical Science and Technology 22 (2008) 1330~1338, Springer

[8] Corke Peter, "Robotics Vision and control, "Fundamental algorithms in MATLAB", Springer.

[9] B.Tondu,"A Theorem of manipulability of redundant serial kinematic chains" Engineering Letters, 15:2, EL_15_2_27, Advance online publication: 17 November 2007

[10] Ryota Ishibashi, ShiSheng Zou, Kazuya Kawaguchi, NaoyukiTakesue, Akira Kojima "A proposal of manipulability based model predictive control for the parallelogram linkage", 10th IFAC Symposium on Robot Control International Federation of Automatic Control September 5-7, 2012. Dubrovnik, Croatia.